,

Study of the Response of the ANTARES Detector instrumented with Direction-Sensitive Optical Modules

M. Anghinolfi, A.Bersani, K. Fratini, M. Osipenko, M. Taiuti
Dipartimento di Fisica dell'Universitá di Genova or Istituto Nazionale di Fisica Nucleare, sezione di Genova, I-16146 Genova, Italy

V. Kulikovsky, A. Plotnikov, E. Shirokov
Institute of Nuclear Physics, Moscow State University, 119899 Moscow, Russia

We studied the performances of the underwater neutrino telescope ANTARES equipped with direction-sensitive optical modules. The main feature of these optical modules is to detect the direction of the incoming Cherenkov light. In this note we show that the effective area of the underwater neutrino telescope ANTARES could be improved at low neutrino energies ($E_\nu < 10$ TeV) by adding in the reconstruction procedure the information on the direction of the detected Cherenkov light.

I. INTRODUCTION

We investigated how the response of the underwater neutrino telescope ANTARES [1] could be improved by introducing the additional information of the direction of the detected Cherenkov light. We designed a prototype of a direction-sensitive optical module (**DOM**) and we accordingly modified the simulation and reconstruction codes [2] currently used by the ANTARES Collaboration to study the response of the detector. The **DOM** is based on a position-sensitive photomultiplier coupled to a light guide system such that all the Cherenkov light arriving from the same direction is focussed on a reduced area of the photocathode. The basic working principles have been discussed in [3]. In Figure 1 it is summarized how the device would work: all photons arriving from the same direction are collected on a single sector of the multi-anodic photomultiplier.

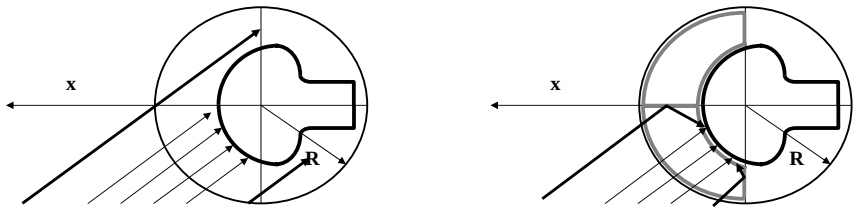

FIG. 1: Left: behaviour of the classical optical module: the Cherenkov light illuminates the whole photocathode surface. Right: the mirrors concentrates the light on a single sector of the photocathode surface.

The realization of a prototype of the direction-sensitive optical is in progress. A cross section of the **DOM** prototype is shown in Figure 2. The prototype is based on a 4-anods 10" photomultiplier position-sensitive. In order to match the refraction index of the photomultiplier and the glass sphere, the volume between the photomultiplier and the glass sphere must be filled with a transparent material like plexiglas or optical gel. A set of mirrors realized with highly reflective 3M plastic material with a reflectivity in the blue region better than silver or aluminum concentrate the light on a single sector of the photocathode surface. Two prototypes of such a photomultiplier have been manufactured by Hamamatsu and the measurement of their optical properties is in progress. We will not discuss in this paper the structure of the **DOM**, but we simply assume that the solid angle (close to 2π) covered by each standard optical module can be subdivided into four independent quadrants. Therefore the new optical module has been implemented in the simulation code using four smaller photomultiplier with reduced angular acceptance. The size of the photocathode area and the cut in the angular acceptance have been defined in order to maintain the same amount of collected light.

The way how the **DOM** has been implemented in the simulation software is discussed in section II; in section III we discuss how we modified the reconstruction program and we show that the response of the telescope based on this solution improves for low energy muons ($E_\mu < 10$ TeV).

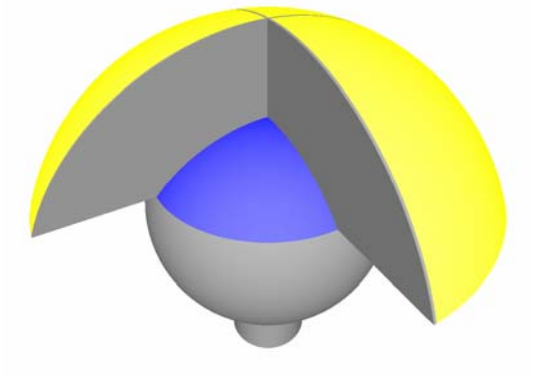

FIG. 2: The prototype of a direction-sensitive optical module based on a 4-anodic photomultiplier coupled to a light-guide system. The main components are the photocathode surface (blue), the mirror system (gray) and the optical gel (yellow).

II. THE RESPONSE OF THE DIRECTION-SENSITIVE OPTICAL MODULE

In this section we briefly verify that the description of the **DOM** is correctly implemented in the simulation program. The standard optical module and the **DOM** configuration have the same sensitive area, therefore the collected light should also be the same. We report in Figure 3 the comparison between the simulations of the amount of light collected with the assumption of zero background (top panel), and with the assumption of 40 kHz background (bottom panel; in Figure 4 the comparison between the number of active optical modules with the assumpion of zero background (top panel), and the same with the assumption of 40 kHz background (bottom panel). The four plots show that there are no differences between the two configurations.

III. THE TELESCOPE RESPONSE

In order to better understand the results, we first remind that the reconstruction program is mainly based on the time response of the photomultipliers. For a given timing value, each active photomultiplier defines in the space an hemi-spherical surface with a thickness proportional to the photomultiplier time resolution as shown in the left panel of Figure 5, representing all the possibile emission points of the detected light.

At least one point of the muon trajectory belongs to the surface and the reconstruction uncertainties clearly increase with the radius of the hemi-spherical surface. For high energy neutrinos ($E_\nu > 10$ TeV) the number of active module is large enough to minimize the uncertainties; but for lower energy neutrino the number of active optical modules decreases and this compensation cannot always occur.

The use of the **DOM** configuration reduces this uncertainty and we anticipate that the effect is particularly evident at neutrino energies smaller than 10 TeV as shown in Figure 9. In fact the surface representing all the possibile emission points of the detected light has now a triangular shape as shown in the right panel of Figure 5. As a consequence, the error on the emission point location is drastically reduced.

The presently available reconstruction software is based on the AART Strategy [4] developed by Aart Heijboer. We included the description of the **DOM** modifying few steps of the recostruction code. To better explain the modification we first summarize the AART Strategy.

A. The AART Strategy

The strategy identifies a reasonable track T_I to be used as the seed for the fit of the data. T_I is estimated by a procedure that includes the following steps: a) the linear fit, b) the M-estimator and c) the fit of the time residuals without noise contribution. As T_I is determined, it is used as input to the final PDF (Probability Density Function) fit that includes the effect of the background.

The AART strategy utilizes for each i-th optical module the local coordinates in the detector, the orientation, the time signal t_i and the collected charge h_i. To better describe the invidual steps of the strategy we now define h_0 the largest hit that provides the reference time t_0 and c_i the flag that identifies the i-th hit that is in coincidence within

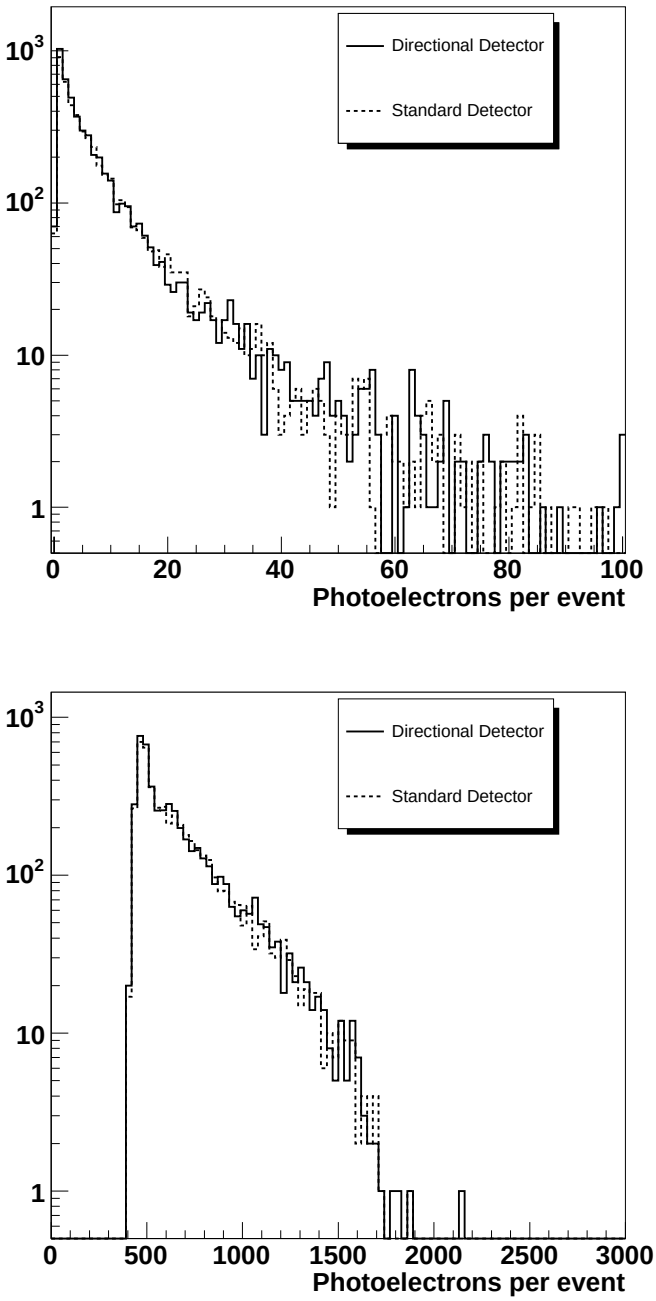

FIG. 3: The comparison between the distributions of the light collected in a single event by a detector equipped with standard optical module (dotted histogram) and with **DOM** (continuous histogram) both with the sensitive area of a 10" photomultiplier with zero background (top panel) and with 40 kHz background (bottom panel).

20 ns with any other hit in nearby photomultiplier. With this definition we allow, in the case of **DOM**, coincidences in the same optical module.

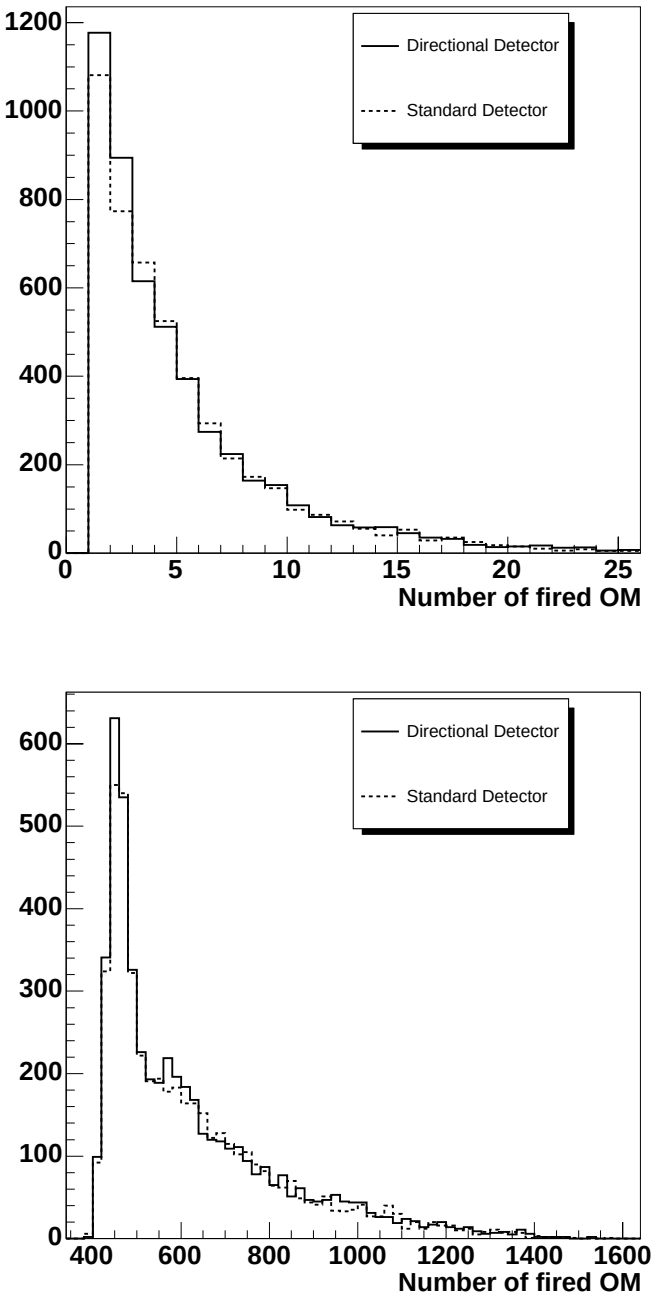

FIG. 4: The comparison between the number of active optical modules in the standard configuration and in the **DOM** one with zero background (top panel) and with 40 kHz background (bottom panel).

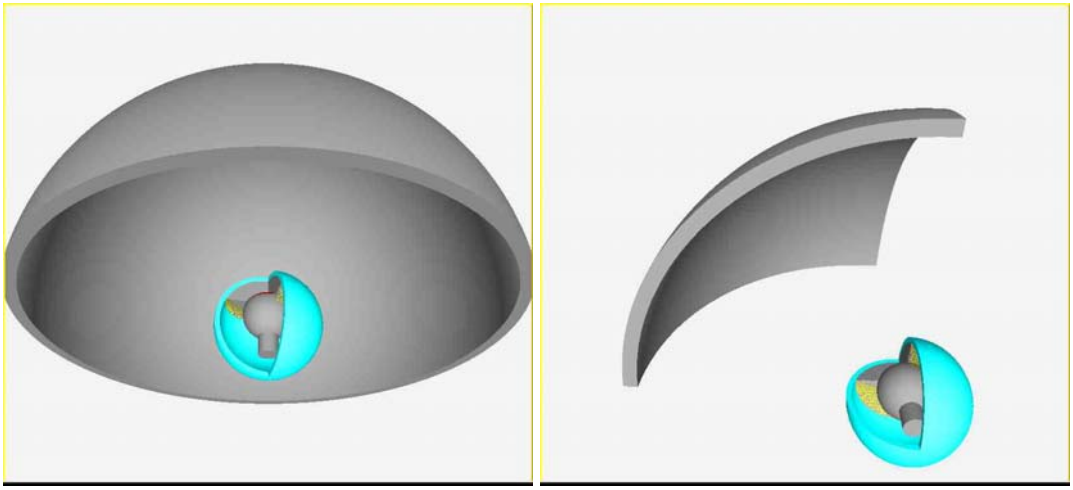

FIG. 5: The graphical description of the location of the possible emission point of the Cherenkov light detected by an optical module at fixed timing. The thickness of the gray region corresponds to the photomultiplier time resolution. Left: standard optical module; right: **DOM**.

B. The Linear Fit

The first step aims to identify a reduced set $\Re_0$ of informations that includes h_0 and all hits h_i that have a time difference $\Delta t_i = t_0 - t_i$ such that the following three constraints are simultaneously satisfied

$$\begin{cases} \frac{distance(h_i,h_0)}{c} - 500 \sum ns < \Delta t_i \\ \frac{distance(h_i,h_0)}{v} - 20\ ns < \Delta t_i \\ distance(h_i,h_0) < 10\ km \end{cases} \tag{1}$$

where c is the muon velocity and v the speed of light in water. This is a reasonally small set of hits that includes most of the signal hits. However the number of noise hits included in $\Re_0$ is too large and therefore a subset $\Re_L$ is derived from $\Re_0$ choosing all hits with

$$h_i > 2.5\ photoelectrons \quad .OR. \quad c_i = .TRUE. \tag{2}$$

The obtained reduced set $\Re_L$ is the input for the linear fit based on the closest approach distance of the muon track compatible with the hits. Assuming the following muon track equation

$$\vec{y}(t) = \vec{p} + \vec{d} \cdot ct \tag{3}$$

the parameters $\vec{p}$ and $\vec{d}$ that define the track are evaluated minimizing the following sum

$$\sum_{i \in \Re_L} \left[\vec{C}_i - \vec{y}(t_i) \right]^2 \tag{4}$$

where the closest approach point $\vec{C}_i$ is evaluated from h_i using a table, defined *a priori,* that connects $\vec{C}_i$ to the hit amplitude, and t_i is the measured time. The output of the linear fit is the track T_L that is then utilized as the starting track of the second step of the reconstruction algorithm.

C. The M-estimator

In order to find the best track, the arrival times of the Cherenkov light $t_i^{th}(T)$, evaluated from a generic track T, are compared to the measured time t_i and the differences (time residuals) $r_i(T) = t_i^{th}(T) - t_i$ minimized. In order

to find a solution T_M almost independent from the starting track T_L the M-estimator fit is applied. It minimizes the following function of the residuals r_i and of the photomultiplier angular acceptance

$$G = \sum_{i \in \Re_M} \left[\kappa \left(-2\sqrt{1 + h_i r_i^2/2} \right) - (1-\kappa) f_{ang}(cos\theta_i) \right] \tag{5}$$

where $\kappa = 0.05$, θ_i is the angle of arrival of the light with respect to the axis of the photumultiplier, and the angular acceptance $f_{ang}(cos\theta_i)$ is reported in Figure 6.

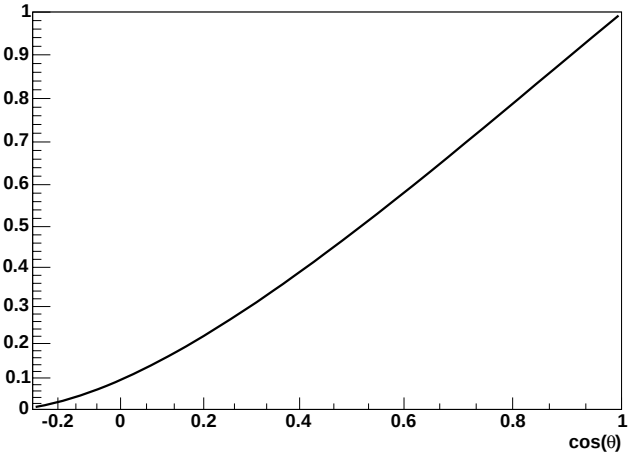

FIG. 6: The standard photomultiplier angular acceptance used in the reconstruction.

The set $\Re_M$ of hits used with the M-estimator fit is the reduced set of $\Re_0$ that satisfies the following constraints

$$\begin{cases} -150\ ns < r_i(T_L) < 150\ ns \\ distance(h_i, T_L) < 100\ m \end{cases} .OR. \quad h_i > 2.3\ photoelectrons \tag{6}$$

D. The Time Residuals Fit

The track T_M obtained from the M-estimator fit is the seed of the likelihood minimization of the Probability Density Function (PDF) $P(t_i|t_i^{th})$ of the residuals r_i, shown in Figure 7 with the assumption of no background. The set $\Re_{\rm PDF}$ of hits used with the PDF-fit is the reduced set of $\Re_M$ that satisfies the following constraints

$$\begin{cases} -0.5\sigma_r < r_i(T_M) < \sigma_r \\ distance(h_i, T_M) < 300\ m \end{cases} \\ .OR. \\ h_i > 2.5\ photoelectrons \\ .OR. \\ c_i = .TRUE. \tag{7}$$

where σ_r is the RMS value of the distribution of the residuals r_i referred to T_M. In order to further reduce the dependence from the starting track T_L, the M-estimator and PDF procedures are repeated several times using different starting tracks T_L' obtained from rotation or translation of the original T_L, producing every time a new T_{PDF} track. The T_{PDF} track that shows the best minimization becomes T_I, input track for the final fit.

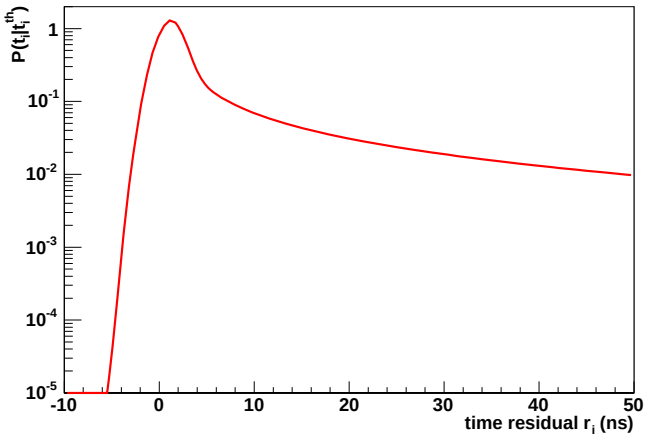

FIG. 7: The Probability Density Function (PDF) used in the reconstruction.

E. The Improved Time Residuals Fit

The final step is based on the likelihood minimization of the improved Probability Density Function (PDF) of the residuals r_i defined as

$$P(t_i|t_i^{th}) = w_{sig}P_{sig}(t_i|t_i^{th}) + (1 - w_{sig})P_{bkg}(t_i|t_i^{th}) \tag{8}$$

where $P_{sig}(t_i|t_i^{th})$ represents the PDF for signal, $P_{bkg}(t_i|t_i^{th})$ represents the PDF for the background noise, and w_{sig}, that depends on the amplitude of the read-out, the orientation and location of the optical module, represents the probability that h_i is a signal hit. The used set $\Re_I$ is the subset of $\Re_0$ that satisfies the following constraints:

$$\begin{cases} -250\ ns < r_i(T_I) < 250\ ns \\ distance(h_i, T_I) < 300\ m \end{cases}$$
$$.OR.$$
$$h_i > 2.5\ photoelectrons \tag{9}$$
$$.OR.$$
$$c_i = .TRUE.$$

F. Implementing the Direction-sensitive Optical Module

The introduction of the direction-sensitive optical module required several changes in the fitting procedure, particularly in the definition of the tables and functions used. First of all the data in the table used in the linear fit have been changed in order to represent the most probable light emission point rather than the closed approach distance. Consequently the linear fit of Eq.(4) has been corrected in order to minimize the light emission point as follows:

$$\sum_i \left[\vec{C}_i - \vec{y}(t_i')\right]^2 \tag{10}$$

where t_i' is obtained from the measured time t_i correcting for the light propagation from the most probable emission point to the optical module.

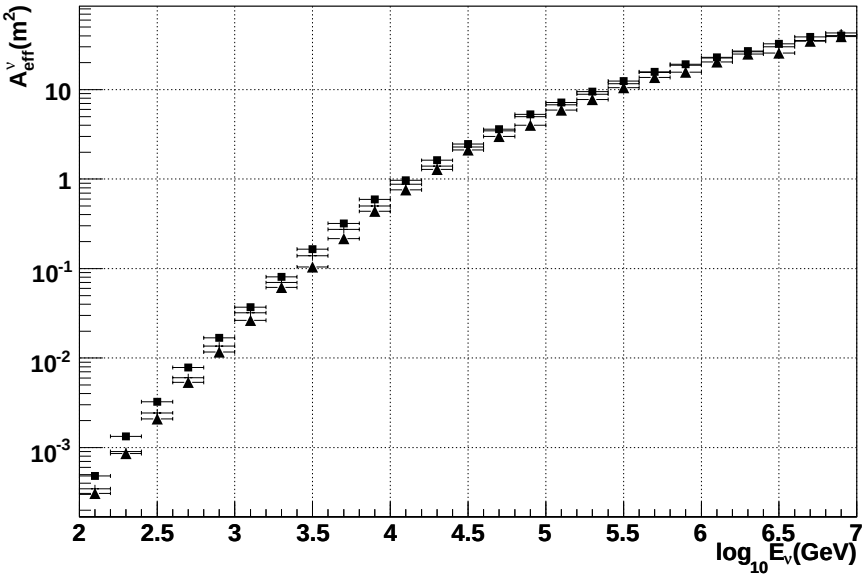

FIG. 8: The effective area of the standard ANTARES detector (crosses) and ANTARES equipped with **DOM** (black squares) for muonic neutrinos assuming $\Delta\theta < 5^{\circ}$. The full triangles represent the result of the standard reconstruction procedure applied to the standard ANTARES detector.

In the simulation and reconstruction programs, the angular acceptance $f_{ang}(cos\theta_i)$ was set equal to that shown in Figure 6 for $cos(\theta) > 0.71$ and equal to zero for $cos(\theta) < 0.71$; and the value of κ has been optimized to 0.01; in the Improved Time Residual Fit the weight w_{sig} has been modified taking into account also the new expected background rate. The value of w_{sig} has been determined from a MonteCarlo simulation as described in the Aart strategy. In addition to the previous modifications we implemented new constraints in order to efficiently use the information of the direction of the detected light and to optimize the response to low energy neutrino. The modifications to the reconstruction program can be summarized as follows:

a) for low energy neutrinos ($E_{\nu} < 100\ TeV$), the average number of hits is small and as a consequence the probability that the highest hit h_0 is generated by the background is not negligible. Therefore, to improve the reconstruction efficiency, h_0 is selected as follows: $h_0 = h_M$ if the largest hit h_M is larger that 3.0 photoelectrons, otherwise h_0 is the largest hit with a coincidence signal (c_M=.TRUE.);

b) after every fitting procedure described in subsections III B to III E, the compatibility between the resulting track and the angular acceptance of the hits used in the reconstruction is verified, the hits not compatible are removed from the set $\Re$ and the fitting procedure is repeated.

c) because in the new geometry the linear fit provides a solution closer to the real track, the range of the rotations used to produce new starting tracks are reduced.

G. ANTARES with the Direction-sensitive Optical Module

We now report the results of the study of the performance of ANTARES equipped with **DOM**. We first consider the simulation and reconstruction of neutrinos with energy below 10^4 GeV because in this energy interval the average number of signal hits is small and the information on the direction of the detected Cherenkov light can improve the reduction of the background contamination.

To study the detector performances we selected the muonic tracks that have been reconstructed with good angular resolution, that is with an angular difference $\Delta\theta$ between the generated and recostructed muon directions better than 5°. This criteria is clearly not appliable in the real measurement because the value of $\Delta\theta$ is intrinsecally unknown. However, this is the first attempt to introduce the directionality in the reconstruction procedure and we decided to begin with a qualitative estimate of the performances, thus postponing the task of finding the best procedure for low energy muons.

In Figure 8 the results for the effective areas of the standard ANTARES detector and ANTARES equipped with **DOM** are reported. For sake of completeness we applied to both geometries the check on the compatibility between the resulting track and the angular acceptance of the hitted photomultiplier. For comparison we show also the results

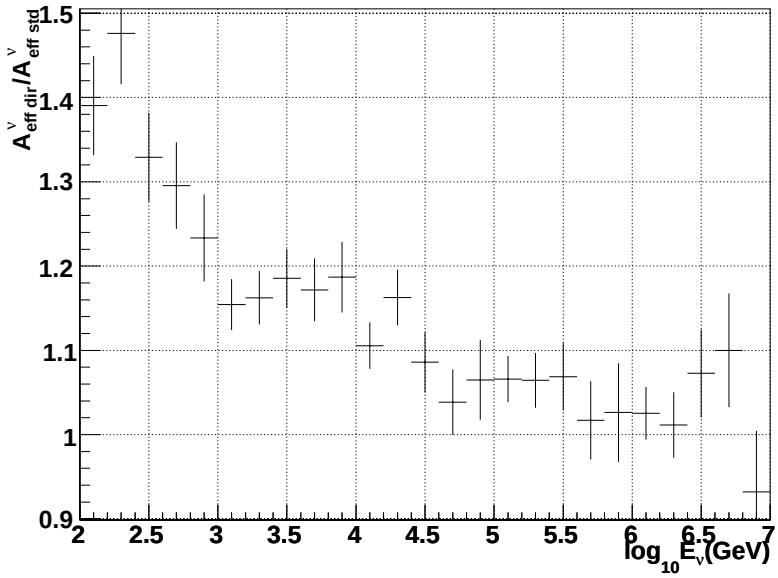

FIG. 9: The ratio of the effective areas of ANTARES equipped with **DOM** and the standard ANTARES detector.

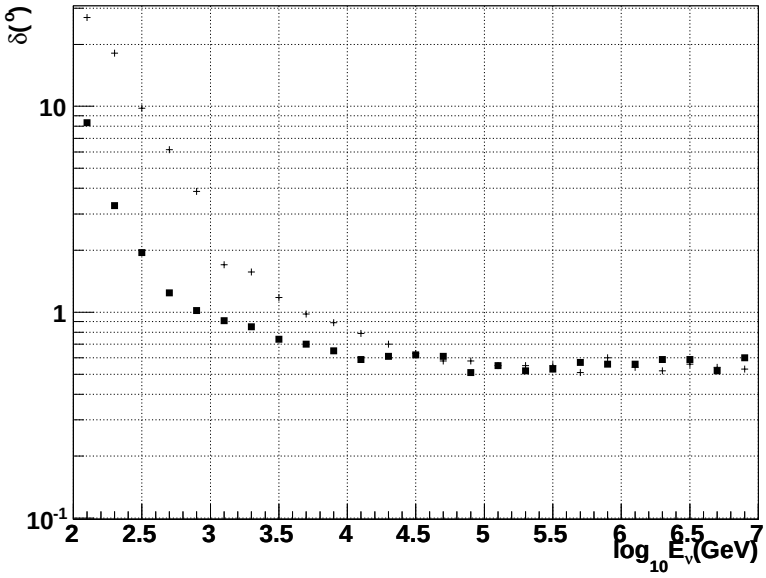

FIG. 10: The median of the angular error $\Delta\theta$ of the muon track reconstruction for the standard ANTARES detector (crosses) and ANTARES equipped with **DOM** (black squares) for all reconstructed muonic neutrinos.

obtained for the standard ANTARES detector reconstructed with the standard reconstruction program. In this case the reconstruction has been done by ... and we only applied the cut $\Delta\theta \leq 5^{\circ}$ to the angular reconstruction. The gain is reported in Figure 9 as the ratio between the effective areas of the two studied configurations: the effective area in the **DOM** configuration improves up to a factor 2 at $E_{\nu} = 100$ GeV and the effect is particularly evident at energies $E_{\nu} < 1$ TeV. The knowledge of the direction of the detected Cherenkov light improves the detector capability to reconstruct the muon trajectories. This is shown in Figure 10 where we show, for all reconstructed trajectories, the comparison between the medians of the angular error $\Delta\theta$ distribution for the standard ANTARES detector and ANTARES equipped with **DOM**. The **DOM** improves the reconstruction accuracy at neutrino energies below 10 TeV.

IV. CONCLUSIONS

We implemented in the Antares reconstruction code, starting from the AART strategy, the algorithm to reconstruct the muon trajectory for a neutrino detector equipped with optical module sensitive to the direction of the detected Cherenkov light. With the modified reconstruction code we simulated the ANTARES geometry instrumented with **DOM** and we compared the performances with those of the standard ANTARES detector. It resulted that:

- the check on the compatibility between the resulting track and the angular acceptance of the hitted photomultiplier increases the quality of the reconstruction;
- the advantage of using the **DOM** consists in a better reconstruction efficiency of the shortest tracks that originate mainly from low energy neutrinos.

---

[1] E. Aslanides *et al.*, the ANTARES proposal, (1999), astro-ph/9907432, `http://antares.in2p3.fr`.
[2] `www.antares2.in2p3.fr` ANTARES-soft Internal notes.
[3] M. Taiuti, Nucl. Instrum. Meth. A **525** (2004) 137.
[4] "An algorithm for track reconstruction in ANTARES" Aart Heijboer ANTARES-soft/20002-002.